18

Vibrations anharmonism effect of solvent OH-groups on IR luminescent properties of semiconductor colloidal quantum dots of lead sulphide

© I.G. Grevtseva, O.V. Ovchinnikov, M.S. Smirnov, K.S. Chirkov, A.N. Latyshev

Voronezh State University,
Voronezh, Russia

e-mail: grevtseva_ig@inbox.ru

Received March 27, 2024
Revised April 11, 2024
Accepted June 14, 2024

The vibrations anharmonism effect of the OH-groups of solvent of the overlap integral of the donor luminescence spectrum KT PbS/2-MPA with the acceptor extinction spectrum (overtones of OH vibrations) showed the Förster radius $R_0 = 0.4$ nm. This value evidences the adsorption of solvent molecules on the QD interfaces during them dissolving in it. In this case, the approximation of the luminescence decay curves of KT PbS/2-MPA QDs demonstrates the greatest agreement with experimental data when the luminescence decay law takes into account the statistical distribution of the number of OH-groups of solvent molecules relative to the QDs. The obtained data indicate the implementation of a dipole-dipole mechanism of non-radiative transfer of electronic excitation energy from KT PbS/2-MPA QDs to the overtones of solvent OH-vibrations, located in the environing volume of QDs.

Keywords: luminescence, quantum yield, luminescence decay time, non-radiative processes, quantum dot, lead sulfide.

DOI: 10.61011/EOS.2024.06.59537.6194-24

Introduction

Creation of IR luminescent sensor materials is important for new photonics technologies and devices, including chemical, biomedical, information and telecommunication technologies, optoelectronics, photocatalysis, etc. [1–6]. Semiconductor colloidal quantum dots (QD) of metal chalcogenides having size-dependent luminescent properties in the region from UV to IR are of great interest for most applications listed above [1–6]. Low luminescence quantum yield of colloidal QD, in particular in case of hydrophilic colloidal solutions, is a serious restrain for practical application [7–10]. It has been found to date that luminescent properties of colloidal QD are defined not only by the electronic structure of the semiconductor and quantum-size effect typical for it, but also by surface environment (passivating ligands, solvents, polymer matrices, etc.) and by the synthesis conditions (precursor concentrations, temperature, pH, etc.) [7–10]. Colloidal synthesis techniques involve QD surface passivation (stabilization) by organic ligands that provide QD solubility and prevent aggregation. Low quantum yields of QD luminescence are often associated with surface defects of a nanocrystal that serve as nonradiative recombination channels. The presence of surface defects is attributed to dangling bonds on the QD surface, chemical properties of the passivating ligand, mechanism of interaction between the ligand and QD, and the presence of reduced or „undercharged" metal atoms on the QD surface [11–18].

Another type of nonradiative processes in colloidal QD involves nonradiative energy transfer (FRET) from electronic excited states of QD to functional molecule groups of surface environment (passivating ligand, solvent, etc.) whose vibrations have significant anharmonicity [19–27]. The influence of the functional groups of solvent molecules has been found for HgTe, CdTe, InAs/CdSe/ZnSe QD [19,23–27]. The authors of [19,23–27] have shown that replacement of hydrogen-containing solvents (water, toluene, etc.) with solvents free of light atoms (deuterated water, trichlorotrifluoroethane, tetrachloromethane, etc.) leads to an increase in quantum yield and IR luminescence decay time of QD. This is attributed to long-wavelength shift of overtone absorption bands and fundamental vibration tones of the functional groups of solvent molecules free of light atoms, and to reduced resonance overlapping of the emitter and quencher. There are few studies of the kind because solvent is often replaced simultaneously with the replacement of passivating ligand. In this case, QD surface state is changed: QD size, concentration of nonradiative and radiative recombination centers, etc. [7,8,11–13,15–17,28]. Deuteration of water solution (D_2O), when absorption of anharmonic vibration overtones of hydroxyl groups may be shifted into the range from 900 nm to 1200 nm, has a considerably lower influence on the electronic structure of QD [24,29].

Such studies were not performed for lead chalcogenide QD (PbS and PbSe), despite the identified decreasing tendency of quantum yield of QD luminescence from 60% to 3% in the range of $0.9-2\,\mu$m with increase in QD size from 3 nm to 10 nm [25,30–32]. The luminescence spectrum of PbS and PbSe QD in this range overlaps significantly with the overtone absorption spectrum of anharmonic OH- and CH-vibrations of solvents. The authors of [25] explain this experimental pattern mainly within FRET from QD to functional groups of hydrophobic ligand

and solvent molecules having overtone absorption bands of C-H-vibrations that feature significant anharmonicity in the range of $1-2\,\mu$m. However, there is still no direct proof of the decrease in the luminescence quantum yield due to nonradiative energy transfer from QD to anharmonic molecular vibrations of the passivator and solvent.

For PbS QD in the range of $0.8-2.0\,\mu$m, results of QD luminescence kinetics investigations are provided separately [33–36]. It is shown that the luminescence decay time decreases from 2.7 to $0.25\,\mu$m as the QD size increases from 2.5 to 9.0 nm [33–36]. Based on the Stokes shift data and temperature dependence of the luminescent properties of PbS QD, the observed size dependence is explained by the existence of quasi-local state whose influence is induced by quantum-size limit only for a particular size of QD [14,33–36]. Moreover, there is theoretical and experimental data that don't fit into this model [10,37–39].

Thus, the existing explanations of the size dependence of spectral luminescent properties, Stokes shift and luminescence mechanism of PbS QD are still controversial [33–39]. In addition, the influence of solvent on the quantum yield of IR luminescence of PbS QD has not been reviewed in detail yet. However, in the near IR range where PbS QD are promising materials for luminescent labeling technologies, biosensorics, optoelectronic devices, etc., the influence of solvent on the QD luminescent properties shall be considered to achieve the priority positions in this field of science and technology.

This study is devoted to determining the influence of anharmonic vibration overtones of the OH-groups of solvent molecules on the quantum yield of IR luminescence of PbS QD when the solvent is changed from H_2O to D_2O.

Materials and research methods

Materials and PbS QD synthesis procedure

Lead nitrate ($Pb(NO_3)_2$), sodium sulfide (Na_2S), 2-Mercaptopropionic acid (2-MPA), sodium hydroxide (NaOH), deuterated water (D_2O), dimethyl sulfoxide (DMSO), indocyanine green (ICG) dye — all chemicals used for this study are of ACS grade.

Colloidal PbS QDs were synthesized by the water synthesis method using the passivating ligand of 2-MPA molecules (hereinafter PbS/2-MPA QD). This synthesis procedure involved mixing 2-MPA (1 mM) and $Pb(NO_3)_2$ (0.5 mM) water solutions at pH 10 followed by addition of Na_2S (0.1 mM) water solution to the reaction mixture. pH of the colloidal solution was controlled by dropwise addition of 1 M NaOH solution. To avoid oxidation of PbS/2-MPA QD at the synthesis stage, nitrogen purging was performed [10,37].

The solvent was replaced by deposition of PbS/2-MPA QD water solution through centrifuge treatment and then the deposit was dissolved in D_2O with retention of the initial colloidal solution volume and QD concentration.

Equipment and research methods

Structural examination of QD was performed by the transmission electron microscopy (TEM) method using the Libra 120 (CarlZeiss, Germany) microscope with digital analysis of the TEM images and X-ray diffraction. The TEM microphotographs were used to find the QD dispersion by sizes in the specimen.

Optical absorption spectra were recorded using the USB2000+ (Ocean optics, USA) spectrometer (in the range of $200-900$ nm) and NIR-Quest (Ocean optics, USA) spectrometer (in the range of $900-2100$ nm), the USB-DT (Ocean optics, USA) was used the radiation source.

Near IR luminescence spectra were recorded using the PDF 10C/M (ThorlabsInc., USA) photodetector with built-in amplifier and a diffraction monochromator with $600\,\text{mm}^{-1}$ grating. The LPC-826 (Mitsubishi, Japan) semiconductor laser diode with 650 nm emission and an optical power of 200 mW was used as a luminescence spectra excitation source.

Quantum yield of luminescence was determined by the relative method:

$$QY = QY_r \frac{I}{I_r} \frac{D_r}{D} \frac{n^2}{n_r^2}, \quad (1)$$

where QY_r is the luminescence quantum yield of the standard, I and I_r is the integral intensity in the luminescence band of QD and the standard, D and D_r are optical densities at the excitation wavelength for PbS/2-MPA QD and the standard (in the experiments D and $D_r \sim 0.1$), n and n_r are the refraction indices of the PbS/2-MPA QD solution and standard, respectively.

H_2O ($n = 1.3314$ at 650 nm at 293 K [40]) and D_2O ($n = 1.3264$ at 650 nm at 293 K [40])B were used as the PbS/2-MPA solvent. ICG dye solution in DMSO with $QY_r = 12\%$ at 800 nm [41] ($n_r = 1.4770$ at 650 nm at 293 K according to the data of [42]) was used as the standard of near IR luminescence quantum yield of PbS/2-MPA QD.

Luminescence decay was investigated using the TimeHarp 260 (PicoQuant, Germany) time-correlated single-photon counting board with the InGaAs KIT-IF-25C (Micro Photon Devices, Italy) single-photon avalanche diode module with a time resolution of 0.5 ns in the spectral region from 900 to 1400 nm. The QD samples were excited by the PICOPOWERLD660 (Alphalas, Germany) semiconductor pulse laser with a wavelength of 660 nm, pulse width of 50 ps and pulse repetition rate of 30 kHz.

Results and discussion

Structural characteristics of PbS QD

Figure 1 shows the TEM images and column diagrams of PbS/2-MPA QD distribution by size in various solvents (H_2O and D_2O). Digital analysis of the TEM images of the PbS/2-MPA QD sample in H_2O has shown that individual spherical nanoparticles with a mean size of about 3 nm and

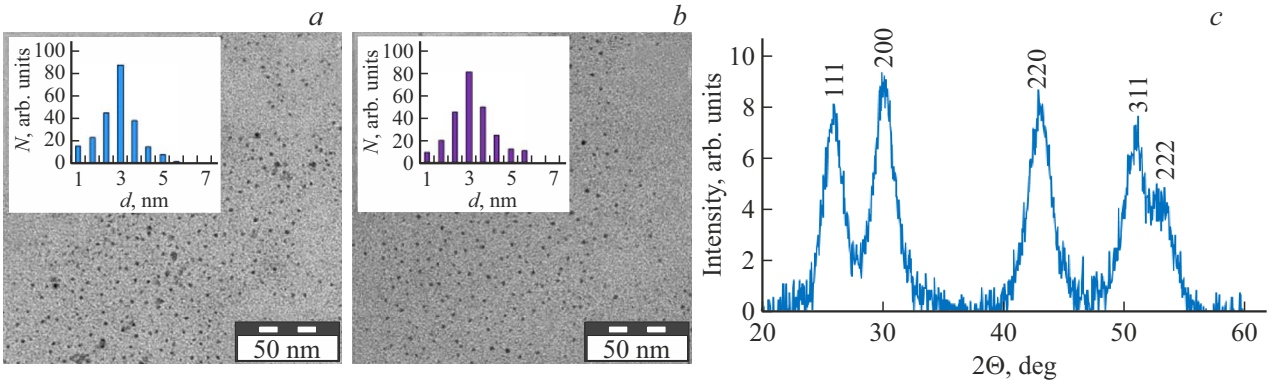

Figure 1. TEM images of PbS/2-MPA QD in H_2O (*a*) and D_2O (*b*). X-ray diffraction of PbS QD in H_2O (*c*).

dispersion not exceeding 20% were formed (Figure 1, *a*). Solvent change from H_2O to D_2O does not lead to significant change in the PbS/2-MPA QD size. According to the TEM images, the mean size of PbS/2-MPA QD in D_2O was equal to 3 nm with dispersion not exceeding 20% (Figure 1, *b*).

The X-ray images of PbS/2-MPA QD in H_2O and D_2O were identical. For the radiation $K_{\alpha Cu}$ with a wavelength of 1.056 Å there are well-defined reflections at 25.9°, 30.1°, 43.05° corresponding to the PbS crystal modification formed in the cubic lattice ($Fm\bar{3}m$) (Figure 1, *c*) [38]. All reflections appeared to be significantly broadened due to the size effect. Crystallite size evaluations conducted using the Debye-Scherrer equation [43,44]

$$d = \frac{0.9\lambda}{\beta \cos\theta}, \qquad (2)$$

where d is the size in nm, λ is the X-ray wavelength, β is the diffraction peak full width at half maximum (peak (220) was used because it didn't overlap with other reflections), θ is the Bragg angle, gave the value of about 3.2 nm, which agrees well with the TEM data.

Thus, the PbS/2-MPA QD samples in H_2O and D_2O are a set of PbS nanocrystals with a mean size of about 3 nm.

Spectral-luminescent properties of PbS QD

Figure 2 shows the optical absorption and luminescence spectra of PbS/2-MPA QD in different solvents (H_2O and D_2O).

The optical absorption spectra at 800 nm has a feature caused by the most probable exciton transition in the optical absorption of PbS/2-MPA QD (Figure 2, curve *1*). Position of this feature is shifted significantly towards shorter wavelengths with respect to the absorption edge of massive PbS/2-MPA (3025 nm (0.41 eV)) [45], which is the demonstration of the quantum-size effect. Solvent change from H_2O to D_2O has no significant influence on the optical absorption spectrum of PbS QD (Figure 2, curves *1*, *2*). Mean size calculation of PbS/2-MPA QD using empirical

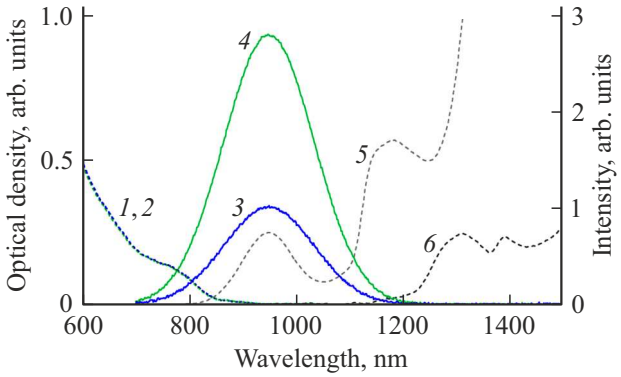

Figure 2. Optical absorption (curves *1*, *2*) and luminescence (*3*, *4*) spectra of PbS/2-MPA QD in H_2O (*1*, *3*) and D_2O (*2*, *4*). Molecular vibration overtone absorption spectra of the H_2O (*5*) and D_2O solvents (*6*).

equation [46]

$$E = 0.41 + \frac{1}{0.0252d^2 + 0.283d}, \qquad (3)$$

where d is the diameter of PbS/2-MPA QD in nm, E is the exciton absorption peak energy, gave the value of 2.7 nm, which agrees well with the TEM and X-ray diffraction data.

The luminescence spectrum of the initial PbS/2-MPA QD sample has a band with a peak at 950 nm and FWHM of 220 nm (Figure 2, curve *3*). The Stokes shift was equal to 0.24 eV, which, according to [37,47], makes it possible assign this peak to the exciton luminescence. Solvent change from H_2O to D_2O leads to the increase in intensity of this luminescence by a factor of 2.5 without any significant transformation of the luminescence spectral band profile of PbS/2-MPA QD (Figure 2, curve *4*). Whereby the luminescence quantum yield of PbS/2-MPA QD increases from 2% to 5% (Figure 2, curves *3*, *4*). The absence of spectral deformations (Stokes shift, spectral profile transformation, etc.) suggests that the QD surface condition remains unchanged when H_2O is changed to D_2O.

Thus, the investigation of luminescent properties of PbS/2-MPA QD in different solvents will make it possible to

QD luminescence decay curve approximation data PbS/2-MPA

Sample	τ_1, μm	a_1	τ_2, μm	a_2	τ_3, μm	a_3	$< \tau >$, μm
PbS (H_2O)	4.50	0.51	0.40	0.29	0.05	0.21	2.40
PbS (D_2O)	7.20	0.83	0.25	0.17	–	–	6.00

identify the influence of vibration anharmonicity of the OH-groups on the luminescence quantum yield of PbS/2-MPA QD in single QD size and unchanged surface conditions.

Figure 2 (curves *5*, *6*) shows the absorption spectra of H_2O and D_2O in the range of 800–1500 nm corresponding to the spectral position of the vibration overtones of the OH- and OD-groups. It can be seen that the absorption decreases almost to zero in case of isotopic substitution of H by D in the range of 800–1200 nm. This is attributed to a significant frequency shift of the fundamental tones (and overtones accordingly) of the stretching and deformation vibrations of the OH-groups to the low-frequency region in case of isotopic substitution of the hydrogen atom (for the OH-groups — $\nu_s^{\mathrm{OH}} = 3261\,\mathrm{cm}^{-1}$, $\nu_{as}^{\mathrm{OH}} = 3351\,\mathrm{cm}^{-1}$, $\delta^{\mathrm{OH}} = 1639\,\mathrm{cm}^{-1}$; for the OD-groups — $\nu_s^{\mathrm{OD}} = 2407\,\mathrm{cm}^{-1}$, $\nu_{as}^{\mathrm{OD}} = 2476\,\mathrm{cm}^{-1}$, $\delta^{\mathrm{OD}} = 1206\,\mathrm{cm}^{-1}$) [24–27].

Thus, the isotopic substitution of H by D in the solvent leads to significant detuning of the spectral resonance of molecular vibration overtone absorption of the solvent and luminescence of PbS/2-MPA QD (950 nm).

The luminescence decay curves of PbS/2-MPA QD in H_2O and D_2O shown in Figure 3, *a* demonstrate the non-exponential behavior that may be attributed to the QD dispersion by sizes and to the presence of quenchers [37,48].

Intrinsic defects of the QD lattice may serve as the luminescence quenchers. They increase the probability of exciton localization, capture charge carriers and may serve as nonradiative recombination centers. Moreover, nonexponentiality of the QD luminescence decay curves is also possible due to the interaction between the electronic system of QD and anharmonic vibration overtones of the OH-groups of the solvent [49,50]. To identify the mean luminescence decay time, the experimental curves were approximated by a sum of several exponents:

$$I(t) = \sum\nolimits_{i=1}^{3} a_i \exp[-t/\tau_i], \tag{4}$$

where a_i and τ_i are the amplitude and time constant of the i-th component (Table).

Analysis of the luminescence decay curves of PbS/2-MPA QD has shown that the mean decay time increased from 2.4 to 6.0 μs during solvent deuteration (Table).

The mean decay time and luminescence intensity data makes it possible to evaluate the efficiency of nonradiative transfer of the electronic excitation:

$$\varphi_1 = 1 - \frac{I_{\frac{\mathrm{PbS}}{\mathrm{H_2O}}}}{I_{\frac{\mathrm{PbS}}{\mathrm{D_2O}}}} = 0.6, \tag{5}$$

$$\varphi_2 = 1 - \frac{\tau_{\frac{\mathrm{PbS}}{\mathrm{H_2O}}}}{\tau_{\frac{\mathrm{PbS}}{\mathrm{D_2O}}}} = 0.6. \tag{6}$$

Coincidence of these values indicates that dynamic luminescence quenching is observed.

Calculation of radiative (k_r) and nonradiative (k_{nr}) recombination constants within the simplest two-level model:

$$k_r = \frac{QY}{< \tau >}, \tag{7}$$

$$k_{nr} = k_r\left(\frac{1 - QY}{QY}\right) \tag{8}$$

has shown that the solution deuteration didn't lead to significant variation of the radiative recombination constant ($k_r^{\mathrm{H_2O}} = 8.3 \cdot 10^3 s^{-1}$ and $k_r^{\mathrm{D_2O}} = 8.2 \cdot 10^3 s^{-1}$). The nonradiative recombination constant decreases by a factor of 2.5 (from $k_{nr}^{\mathrm{H_2O}} = 4 \cdot 10^5 s^{-1}$ to $k_{nr}^{\mathrm{D_2O}} = 1.6 \cdot 10^5 s^{-1}$). The identified decrease in luminescence intensity and decay time in H_2O compared with D_2O and the growth of the nonradiative recombination constant indicate the nonradiative transfer of the electronic excitation energy from PbS/2-MPA QD to the OH-groups of H_2O solvent. The absence of changes in the radiative recombination constant as the luminescence quantum yield of PbS/2-MPA QD increases during replacement of H_2O by D_2O supports the previous conclusion on the QD structure constancy:

Employment of the sum of several exponents for description of the luminescence decay pattern of PbS/2-MPA QD does not reveal the energy transfer mechanism [50]. Additional information on the mechanism of nonradiative energy transfer from PbS/2-MPA QD to the OH-groups was obtained by approximation of the luminescence decay kinetics using R. Kohlrausch's exponential function [49,50]:

$$I_D(t) = I_D(0) \exp\Big[-\frac{t}{\tau_D} - 2b\Big(\frac{t}{\tau_D}\Big)^{\beta}\Big], \tag{9}$$

where I_D and τ_D are the donor luminescence intensity and decay time; b — is the constant depending on the distance between the donor and acceptor, β is some parameter whose value is indicative of the electronic excitation energy transfer mechanism [49].

For the FRET dipole-dipole mechanism, $\beta = 0.5$. Such situation, in turn, corresponds to random distribution by the donor (QD) and acceptor (H_2O molecules) distances within the three-dimensional medium [49]. Approximations of the luminescence decay curve of PbS/2-MPA QD in H_2O by function (9) are shown in Figure 3, *b*. It can be seen that function (9) has significant deviations from the experimental decay curve of PbS QD in H_2O.

Actually, when PbS/2-MPA QD are dissolved in water, the water molecules appear to be adsorbed on the surface of PbS/2-MPA QD. In this case, the function from [50,51] shall be used for approximation of the luminescence decay curves. This function implies that the number of quenchers per each energy donor is distributed according to the Poisson law. The quenching rate (energy transfer rate) per

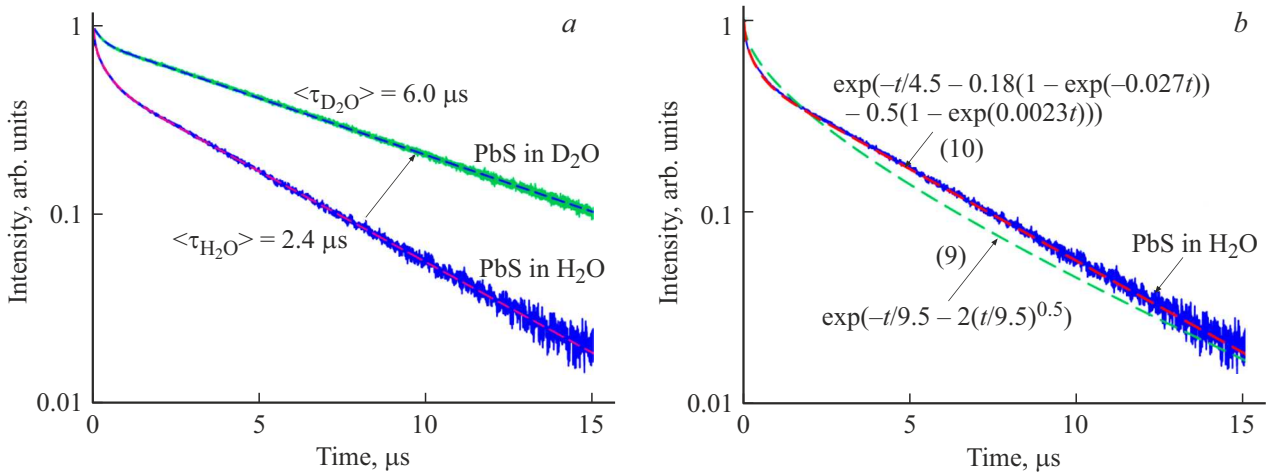

Figure 3. (*a*) Experimental curves of the luminescence decay kinetics of PbS/2-MPA QD in H_2O and D_2O (curves of approximation by a sum of several exponents are shown dashed (4)). (*b*) Approximation of the decay curve of PbS/2-MPA QD in H_2O by R. Kohlrausch's (9) and M. Tachiya's (10) functions.

each quencher is defined only by the number of quenchers. In such case, the luminescence decay curves shall be described by M. Tachiya's function [50,51]:

$$I_D(t) = I_D(0)\exp\Big[-\frac{t}{\tau_D} - < n_1 > (1-\exp[k_1 t]) - < n_2 > (1-\exp[k_2 t])\Big], \quad (10)$$

where $< n_{1,2} >$ is the mean number of two types of quenchers per QD; $k_{1,2}$ are the constants of energy transfer from QD to the solvent molecules. High confidence of the approximation was achieved when two types of quenchers were considered, for example, the OH-groups of the water molecules on the internal and external QD coordination spheres. Description of the experimental luminescence decay curves of PbS/2-MPA QD in H_2O through expression (10) explains the experimental data most precisely (Figure 3, *b*).

Despite the empirical facts indicating the nonradiative energy transfer from PbS QD to anharmonic vibrations of the H_2O molecules, the dipole-dipole energy transfer mechanism remains tentative. Let's evaluate the Forster radius in the dipole-dipole mechanism assumption [52]:

$$R_0 = \Big[8.875\cdot 10^{-25}\chi^2 n^{-4} QY^{\mathrm{PbS}} \frac{\int I_{\mathrm{lum}}^{\mathrm{PbS}}(\lambda)\varepsilon(\lambda)\lambda^4 d\lambda}{\int I_{\mathrm{lum}}^{\mathrm{PbS}}(\lambda)d\lambda}\Big]^{\frac{1}{6}}, \quad (11)$$

where $n = 1.33$ is the refractive index of water, χ^2 is the spatial factor equal to 0.475, QY^{PbS} is the luminescence quantum yield of PbS/2-MPA QD in D_2O, $I_{\mathrm{lum}}^{\mathrm{PbS}}(\lambda)$ is the radiation spectrum of PbS/2-MPA QD — the energy donor, $\varepsilon(\lambda)$ $[1\cdot \mathrm{M}\cdot \mathrm{cm}^{-1}]$ is the molar extinction coefficient of the energy acceptor H_2O. The Forster radius appeared to be equal to $R_0 = 0.4$ nm, which is indicative of water molecule adsorption on the PbS/2-MPA QD surface.

The energy transfer efficiency expression allows the mean distance between the donor and acceptor r to be calculated using the Forster radius:

$$\varphi = \frac{R_0^6}{R_0^6 + r^6}. \quad (12)$$

r for PbS QD in H_2O appeared to be equal to 0.37 nm. The resulting distance r actually corresponds to the mean distance from QD to the water molecule taking into account the size of the passivating ligand molecules ($\sim 0.4 - 0.5$ nm).

Thus, the obtained experimental patterns prove the nonradiative dipole-dipole energy transfer of the electronic excitation from PbS/2-MPA QD to the anharmonic molecular vibrations of the solvent (H_2O).

Conclusion

The study describes the empirical patterns demonstrating the influence of the anharmonic vibrations of the OH-groups of the solvent molecules on the near IR luminescence quantum yield of colloidal PbS/2-MPA QD. Solution deuteration leads to significant offset of the OD-vibration overtone absorption bands (1315 nm) from the luminescence band of PbS/2-MPA QD (950 nm) without affecting considerably the QD surface condition. In this case, the growth of the luminescence quantum yield of PbS/2-MPA QD from 2% to 5% is observed with simultaneous increase in the luminescence decay time rom 2.4 to 6.0 μs and decrease in the nonradiative recombination constant by a factor of 2.5.

The analysis of the luminescence decay curve approximations of PbS/2-MPA QD has shown that the maximum agreement with the experimental data is observed when the luminescence decay law considers the statistical distribution by the number of the OH-groups of the solvent molecules

with respect to QD. Numerical calculations of the integral of the donor (PbS/2-MPA QD) luminescence spectrum overlapping with the acceptor (OH-vibration overtones) extinction spectrum gave the Forster radius $R_0 = 0.4$ nm, which corresponds to the solvent molecule adsorption on the QD surface when QD are dissolved in the solvent. The mean distance between the donor and acceptor within the FRET theory has shown good agreement with the mean distance from QD to the water molecule that depends on the molecule size of the 2-MPA passivating ligand and concentration of quenchers (H_2O molecules) in the solution ($\sim 0.4 - 0.5$ nm).

Thus, the obtained data supports the implementation of the dipole-dipole mechanism of nonradiative electronic energy transfer from PbS/2-MPA QD to the OH-vibration overtones of the solvent that are located in the QD environment. The identified experimental patterns are of practical value because consideration of the solvent influence on the IR luminescence quantum yield of QD is important for creation of effective luminescence labeling systems, biosensorics, optoelectronic devices, etc.

Acknowledgments

Transmission electron microscopy results were obtained using the Libra 120 microscope provided by the Shared Use Center of „Voronezh State University“.

Funding

This study was funded by the Russian Science Foundation as part of research project № 22-72-00098.

Conflict of interest

The authors declare that they have no conflict of interest.

References

[1] Yu Ma, Yu Zhang, W.W. Yu. J. Mater. Chem. C, **7**, 13662 (2019). DOI: 10.1039/C9TC04065J
[2] H.M. Gil, T.W. Price, K. Chelani, J.-S.G. Bouillard, S.D.J. Calaminus, G.J. Stasiuk. iScience, **24** (3), 102189 (2021). DOI: 10.1016/j.isci.2021.102189
[3] M. Han, O. Karatum, S. Nizamoglu. ACS Appl. Mater. Interfaces, **14**, 18, 20468 (2022). DOI: 10.1021/acsami.1c25009
[4] L. Seravalli. Microelectronic Engineering, **276**, 111996 (2023). DOI: 10.1016/j.mee.2023.111996
[5] C.L. Phillips, A.J. Brash, M. Godsland, N.J. Martin, A. Foster, A. Tomlinson, R. Dost, N. Babazadeh, E.M. Sala, L. Wilson, J. Heffernan, M/S. Skolnick, A.M. Fox. Sci Rep., **14**, 4450 (2024). DOI: 10.1038/s41598-024-55024-6
[6] A.A.H. Abdellatif, M.A. Younis, M. Alsharidah, O. Al Rugaie, H.M. Tawfeek. Challenges and Clinical Potential. Int. J. Nanomedicine, **17**, 1951 (2022). DOI: 10.2147/IJN.S357980
[7] D. Pluta, H. Kuper, R.T. Graf, Ch. Wesemann, P. Rusch. Nanoscale Adv., **5**, 5005 (2023). DOI: 10.1039/D3NA00404JJ [Zhou, F. Ma, K. Chen, W. Zhao, R. Yang, Ch. Qiao, H. Shen, W.-Sh. Su, M. Lu, Yu. Zheng, R. Zhang, L. Chena, S. Wang. Nanoscale Adv., **5**, 3896 (2023) DOI: 10.1039/D3NA00251A].
[8] A. Olejniczak, R. Rich, Z. Gryczynski, B. Cichy. Nanoscale Horiz., **7**, 63 (2022) DOI:10.39/D1NH00424G
[9] I.G. Grevtseva, K.S. Chirkov, O.V. Ovchinnikov, M.S. Smirnov. Inorganic Materials, **59** (10), 1045 (2023). DOI: 10.1134/S0020168523100047
[10] I.G. Grevtseva, O.V. Ovchinnikov, M. S.Smirnov, T.S. Kondratenko, V.N. Derepko, A.M.H. Hussein, N.E. Egorov, E.A. Vozgorkova. Opt. Spectrosc., **130** (12), 1910 (2022). DOI: 10.21883/OS.2022.12.54100.4106-22
[11] M.S. Smirnov, O.V. Ovchinnikov, I.G. Grevtseva, A.I. Zvyagin, A.S. Perepelitsa, R.A. Ganeev. Opt. Spectrosc., **124** (5), 681 (2018). DOI: 10.1134/S0030400X18050211
[12] V.A. Krivenkov, P.S. Samokhvalov, P.A. Linkov, D.O. Solovyeva, G.E. Kotkovskii et al. SPIE, **9126**, 91263 (2014). DOI: 10.1117/12.2057828
[13] J.E. Lewis, X.J. Jiang. Nanotechnology, **21**, 455402 (2010). DOI: 10.1088/0957-4484/21/45/455402
[14] I. Fosse, S. Lal, A.N. Hossaini, I. Infante, A.J. Houtepen. J. Phys. Chem. C, **125**, 23968 (2021). DOI: 10.1021/acs.jpcc.1c07464
[15] S. Aynehband, M. Mohammadi, K. Thorwarth, R. Hany, F.A. Nuesch, M.D. Rossell, R. Pauer, J.-M. Nunzi, A. Simchi. ACS Omega, **5** (25), 15746 (2020). DOI: 10.1021/acsomega.0c02319
[16] P. Papagiorgis, D. Tsokkou, K. Gahlot, L. Protesescu, A. Manoli, F. Hermerschmidt, C. Christodoulou, S.A. Choulis, M.V. Kovalenko, A. Othonos, G. Itskosl. J. Phys. Chem. C, **124** (50), 27848 (2020). DOI: 10.1021/acs.jpcc.0c09790
[17] M. Debayle, T. Marchandier, X. Xu, N. Lequeux, T. Pons. ACS Appl. Materials & Interfaces, **11** (28), 25008 (2019). DOI: 10.1021/acsami.9b06194
[18] V.L. Ermolaev. Opt. Spectrosc., **125** (2), 256 (2018). DOI: 10.21883/OS.2018.08.46368.97-18
[19] E.B. Sveshnikova, V.L. Ermolaev. Opt. Spectrosc., **111** (1), 34 (2011). https://elibrary.ru/download/elibrary_16525621_62511575.pdf
[20] V.L. Ermolaev, E.B. Sveshnikova, E.N. Bodunov. Physics-Uspekhi, **39** (3), 261 (1996). DOI: 10.3367/UFNr.0166.199603c.0279
[21] V.L. Ermolaev, E.B. Sveshnikova, T.A. Shakhverdov. Rus. Chem. Rev., **44** (1), 48 (1975). https://www.uspkhim.ru/RCR2142pdf
[22] A. Aharoni, D. Oron, U. Banin, E. Rabani, J. Jortner. Phys. Rev. Lett., **100**, 057404 (2008). DOI: 10.1103/PhysRevLett.100.057404
[23] Q. Wen, St.V. Kershaw, S. Kalytchuk, O. Zhovtiuk, C. Reckmeier. ACS Nano, **10** (4), 4301 (2016). DOI: 10.1021/acsnano.5b07852
[24] O.E. Semonin, J.C. Johnson, J.M. Luther, A.G. Midgett, A.J. Nozik, M.C. Beard. J. Phys. Chem. Lett., **1**, 2445 (2010). DOI: 10.1021/jz100830r
[25] S.E. Lappi, B. Smith, S. Franzen. Spectrochim. Acta, Part A, **60**, 2611 (2004). DOI: 10.1016/j.saa.2003.12.042
[26] S. Klingler, J. Hniopek, R. Stach, M. Schmitt, J. Popp. ACS Meas. Sci. Au, **2** (2), 157 (2022). DOI: 10.1021/acsmeasuresciau.1c00048

[27] B. Xue, J. Cao, D. Deng, J. Xia, J. Jin, Zh. Qian, Yu. Gu. J. Mater. Sci: Mater Med., **23**, 723 (2012). DOI: 10.1007/s10856-012-4548-z
[28] S.I. Sadovnikov, A.I. Gusev. RSC Adv., **10**, 40171 (2020). DOI: 10.1039/D0RA07853K
[29] H. Du, C. Chen, R. Krishnan, T.D. Krauss, J.M. Harbold, F.W. Wise, M.G. Thomas, J. Silcox. Nano Lett., **2** (11), 1321 (2002). DOI: 10.1021/nl025785g
[30] H. Liu, P. Guyot-Sionnest. J. Phys. Chem. C, **14** (35), 14860 (2010). DOI: 10.1021/jp105818e
[31] B.L. Wehrenberg, C. Wang, P. Guyet-Sionnest. J. Phys. Chem. B, **106**, 10634 (2002). DOI: 10.1063/1.4917388
[32] P.S. Parfenov, A.P. Litvin, A.V. Baranov, E.V. Ushakova, A.V. Fedorov, A.V. Prudnikovb, M.V. Artemyev. Opt. Spectrosc., **112**, 868 (2012). DOI: 10.1134/S0030400X12060136
[33] A.P. Litvin, P.S. Parfenov, E.V. Ushakova, A.L. Simoes Gamboa, A.V. Fedorov et al. J. Phys. Chem. C, **118** (35), 20721 (2014). DOI: 10.1021/jp507181k
[34] C. Cheng, J. Li, X. Chengb. J. Lumin., **188**, 252 (2017). DOI: 10.1016/j.jlumin.2017.04.037
[35] E.V. Ushakova, A.P. Litvin, P.S. Parfenov, A.V. Fedorov, M. Artemyev, A.V. Prudnikau, I.D. Rukhlenko, A.V. Baranov. ACS Nano, **6** (10), 8913 (2012). DOI: 10.1021/nn3029106
[36] I. Grevtseva, T. Chevychelova, O. Ovchinnikov, M. Smirnov, T. Kondratenko, V. Khokhlov, A.I. Zvyagin, M. Astashkina, K. Chirkov. Optical and Quantum Electronics, **55** (5) (2023). DOI: 10.1007/s11082-023-04658-3
[37] M.S. Gaponenko, A.A. Lutich, N.A. Tolstik, A.A. Onushchenko, A.M. Malyarevich, E.P. Petrov, K.V. Yumashev. Phys. Rev. B, **82**, 125320 (2010). DOI: 10.1103/PhysRevB.82.125320
[38] Dae Gwi Kim, T. Kuwabara, M. Nakayama. J. Lumin., **119–120**, 214 (2006). DOI: 10.1016/j.jlumin.2005.12.033
[39] S. Kedenburg, M. Vieweg, T. Gissibl, H. Giessen. Opt. Mater. Express, **2**, 1588 (2012). DOI: 10.1364/OME.2.001588
[40] F.W.B. van Leeuwen, B. Cornelissen, F. Caobelli, L. Evangelista, L. Rbah-Vidal, S. Del Vecchio, C. Xavier, J. Barbet, M. de Jong. EJNMMI Radiopharm. Chem., **2**, 15 (2017). DOI: 10.1186/s41181-017-0034-8
[41] O. Ciocirlan, O. Iulian. J. Serb. Chem. Soc., **74** (3), 317 (2009). DOI: 10.2298/JSC0903317C
[42] L.V. Vu, S.C. Doanh, L.T. Nga, N.N. Long. e-J. Surf. Sci. Nanotech., **9**, 494 (2011). DOI: 10.1380/ejssnt.2011.494
[43] P. Scherrer. Nachr. Ges. Wiss. Gott., **26**, 98 (1918).
[44] W.W. Scanlon. J. Phys. Chem. Solids, **8**, 423 (1959). DOI: 10.1016/0022-3697(59)90379-8
[45] I. Moreels, K. Lambert, D. Smeets, D. Muynck, T. Nollet, J.C. Martins, F. Vanhaecke, A. Vantomme, Ch. Delerue, G. Allan, Z. Hens. ACS Nano, **3** (10), 3023 (2009). DOI: 10.1021/nn900863a
[46] J.R. Caram, S.N. Bertram, H. Utzat, W.R. Hess, J.A. Carr, T.S. Bischof, A.P. Beyler, M.W.B. Wilson, M.G. Bawendi. Nano Lett., **16** (10), 6070 (2019). DOI:10.1021/acs.nanolett.6b02147
[47] S. Sadhu, M. Tachiya, A. Patra. J. Phys. Chem. C, **114** (6), 2842 (2010). DOI: 10.1021/jp912268m
[48] E.N. Bodunov, V.V. Danilov, A.S. Panfutova, A.L. Simoes Gamboa. Ann. Phys. (Berlin), **528** (3–4), 272 (2016). DOI: 10.1002/andp.201500350
[49] M.S. Smirnov. Opt. Spectrosc., **123** (5), 705 (2017). DOI: 10.1134/S0030400X17090284
[50] M. Tachiya. Chem. Phys. Lett., **33** (2), 289 (1975). DOI: 10.1016/0009-2614(75)80158-8
[51] F.G. Sanchez, C.C. Ruiz. J. Lumin., **69**, 179 (1996). DOI: 10.1016/S0022-2313(96)00116-0

Translated by E.Ilinskaya